Structural Homology of the Central Conserved Region of the Attachment Protein G of Respiratory Syncytial Virus with the Fourth Subdomain of 55-kDa Tumor Necrosis Factor Receptor

Johannes P. M. Langedijk,*,[1] Bert L. de Groot,† Herman J. C. Berendsen,† and Jan T. van Oirschot*

*Department of Mammalian Virology, Institute for Animal Science and Health (ID-DLO), P.O. Box 65, 8200 AB, Lelystad, The Netherlands; and †Department of Biophysical Chemistry, University of Groningen, Nijenborgh 4, 9747 AG Groningen, The Netherlands

The attachment protein G of respiratory syncytial virus (RSV) has a modular architecture. The ectodomain of the protein comprises a small folded conserved region which is bounded by two mucin-like regions. In this study, a sequence and structural homology is described between this central conserved region of RSV-G and the fourth subdomain of the 55-kDa tumor necrosis factor receptor (TNFr). The three-dimensional structures of RSV-G and human TNFr were previously determined with NMR spectroscopy and X-ray crystallography, respectively. The C-terminal part of both subdomains fold into a cystine noose connected by two cystine bridges with the same spacing between cysteine residues and the same topology. Although a general structural similarity is observed, there are differences in secondary structure and other structural features. Molecular Dynamics calculations show that the BRSV-G NMR structure of the cystine noose is stable and that the TNFr crystal structure of the cystine noose drifts towards the BRSV-G NMR structure in the simulated solution environment. By homology modelling a model was built for the unresolved N-terminal part of the central conserved region of RSV-G. The functions for both protein domains are not known but the structural similarity of both protein domains suggests a similar function. Although the homology suggests that the cystine noose of RSV-G may interfere with the antiviral and apoptotic effect of TNF, the biological activity remains to be proven.   © 1998 Academic Press

Key Words: TNFr; RSV; Molecular Dynamics; homology modeling; cystine noose.

Infections with respiratory syncytial virus (RSV) are a major cause of respiratory tract disease in humans, cattle, sheep and goats (Stott and Taylor, 1985). These viruses are classified within the *Pneumovirus* genus of the *Paramyxoviridae.* The *Paramyxoviridae* comprise enveloped viruses which contain two envelope glycoproteins, the fusion protein (F) and the attachment protein. The attachment protein (G) of RSV is heavily glycosylated and highly variable and shares neither sequence nor structural homology with attachment proteins of other paramyxoviridae (Satake *et al.,* 1985; Wertz *et al.,* 1985). RSV-G exists as an anchored type II membrane protein and as a smaller soluble form that is secreted into the medium (Hendricks *et al.,* 1987; Roberts *et al.,* 1994). The ectodomain of the protein has a modular architecture and comprises a small folded conserved region which is bounded by two mucin-like regions (Langedijk *et al.,* 1996a). This central conserved region is an important antigenic site in bovine (B)RSV-G (Langedijk *et al.,* 1996a, 1996b, 1997a) and human (H)RSV-G (Norrby *et al.,* 1987; Langedijk *et al.,* 1997b). Immunization with a peptide corresponding to the C-terminal part of the central conserved region induced protection from HRSV-A infection and a monoclonal antibody directed against the peptide was able to confer passive protection from challenge (Simard *et al.,* 1997; Trudel *et al.,* 1991). NMR analysis showed that the C-terminal part of the central conserved region of BRSV-G folds as a cystine noose connected by two disulfide bridges (Doreleijers *et al.,* 1996).

In this study, a sequence and structural homology of the central conserved region of RSV-G with the fourth subdomain of the 55-kDa tumor necrosis factor receptor (TNFr) is described. All TNFr-like proteins comprise several repeating TNFr subdomains. Although the overall sequence similarity between the repeats is low, most of these homologous TNFr modules contain 6 Cys residues forming supposedly disulfide bridges within the module. The C-terminal half of the fourth repeat is atypical and structurally different from the other three repeats of the 55-kDa TNFr (Naismith *et al.,* 1996) (Fig. 1). Moreover, the primary sequence is inconsistent with all other known TNFr-like repeats.

The four subdomains of the 55-kDa TNFr are made up of repeats of three distinct small modules termed A1, B2 and C2 (Naismith *et al.,* 1996) (Fig. 1). Each subdomain contains two tightly packed modules. The N-terminal A1 module has an S-shape fold and contains one cystine bridge. The C-terminal part of the subdomain is mostly a

TABLE 1

Sequence Alignments between Central Conserved Regions of RSV-Gs and Fourth Subdomains of 55-kDa TNFrs[a]

		Sequence
HRSV-G, type A	(159–186)	P N N D F H *F E V* . F N F *V P C S I C S N N P T C W A I C*
HRSV-G, type B	(159–186)	P K D D Y H *F E V* . F N F *V P C S I C G N N Q L C K S I C*
BRSV-G	(159–186)	H Q D H N N *F Q T* . L P Y <u>*V P C S T C E G N L A C L S L C*</u>
ORSV-G	(159–186)	Q Q D Y S D *F Q I* . L P Y *V P C N I C E G D S A C L S L C*
55kD TNFr mouse	(139–166)	C . H A G F *F L R E S E C V P C S H C K K N E E C M K L C*
55kD TNFr rat	(139–166)	C . H A G F *F L S G N E C T P C S H C K K N Q E C M K L C*
55kD TNFr human	(139–166)	C . H A G F *F L R E N E C* <u>*V S C S N C K K S L E C T K L C*</u>
55kD TNFr swine	(139–166)	C . H S G F *F L R D K E C V S C V N C K* . *N A D C K N L C*

[a] Bold-faced characters are conserved between RSV-G and 55kD TNFr. The sequences that are used for the simulations are underlined.

B2 module which folds up-down-up and contains one or two cystine bridges. However, in the fourth subdomain the C-terminal part is a C2 module that folds in a cystine noose which contains two cystine bridges similar to the cystine noose of BRSV-G (Naismith *et al.*, 1996; Doreleijers *et al.*, 1996). The significance of this structural homology is studied by Molecular Dynamics. Based on this homology, a detailed 3-D model for the complete central conserved region of RSV-G is proposed.

RESULTS

Sequence similarity

When the complete primary structure of BRSV-G was used to search in the sequence databases for homologous proteins, not one sequence was found with any obvious similarity, apart from the RSV-G sequences. However, the modular protein architecture allowed for a more directed homology search that was limited to the discrete central conserved region (Langedijk *et al.*, 1996a). The similarity search for this small region revealed the highest homology with a small region of the 55-kDa tumor necrosis factor receptor (TNFr) (Table 1). Although the similarity seemed just a local homology over a short amino acid stretch of the 55-kDa TNFr, the similarity is actually a high global homology when the homologous TNFr sequence was compared with the crystal structure of TNFr (Banner *et al.*, 1993; Naismith *et al.*, 1996). That is, the sequence similarity corresponds to the fourth subdomain of four subdomain repeats that make up the ectodomain of the 55-kDa TNFr (Fig. 1). The alignment of the complete central conserved region of RSV-G with the fourth TNFr subdomain shows that both regions have the same length. Moreover, the complete central conserved region of RSV-G and the complete fourth TNFr-subdomain have important similarities (Table 1).

The number of identical amino acids between the central conserved region of bovine RSV-G, ovine RSV-G and human RSV-G is comparable to the number of identical amino acids between the central conserved region of RSV-G and the fourth mouse TNFr subdomain (Table 1). Although the central conserved region of RSV-G is the most conserved extracellular part of the protein, only a small number of residues are conserved in all known central conserved

regions of RSV-G. The four cysteine residues, Val_{171}, Pro_{172}, Ser_{174}, Asn_{179} and Leu_{185} that are conserved in the central conserved region of RSV-G are also present in the fourth subdomain of mouse 55-kDa TNFr.

Structural similarity

The three-dimensional structures of the C-terminal part of the central conserved region of BRSV-G and the
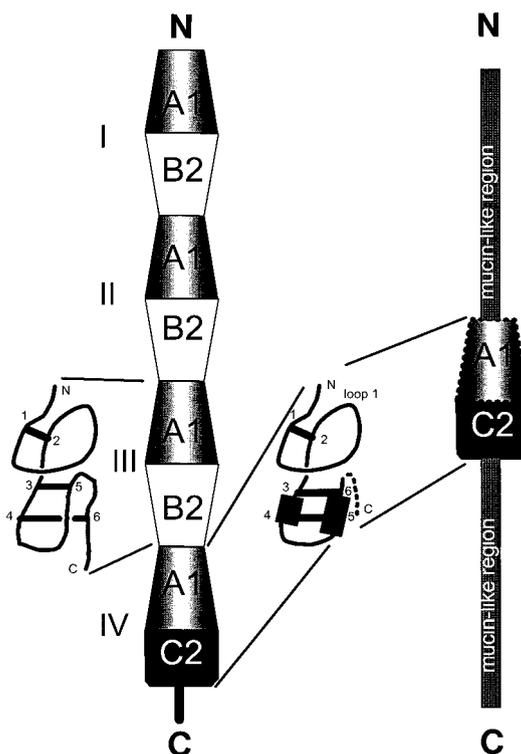
FIG. 1. Schematic representation of the ectodomains of 55-kDa TNFr (left) and RSV-G (right). For the TNFr, the four repeats are indicated with large roman numerals. Modules with similar structure are indicated with different fills. RSV-G is highly schematically presented as a A1C2 domain between two mucin-like regions. C2 is the cystine noose. The structure of the proposed A1 module is hypothetical for RSV-G. The schematic folds for the modules are indicated and the cysteine residues are numbered. Helices in cystine noose are denoted by black rectangles. The disulfide bridges are represented by thick lines. The first disulfide bridge in loop 1 of the A1 module is replaced by His_{159} and Tyr_{170} in BRSV-G. N and C terminus are marked by N and C, respectively.
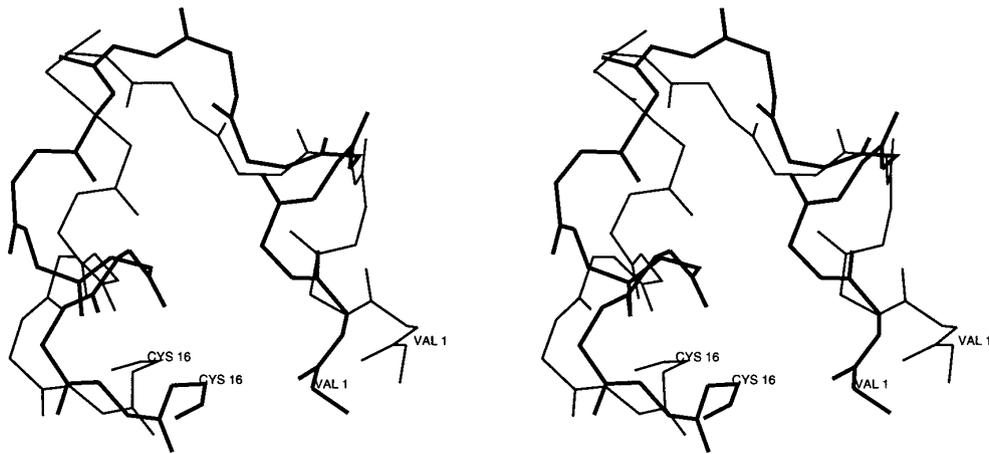
FIG. 2. Stereo representation of the superposition of cystine nooses of BRSV-G (thick line) and hTNFr (thin line).

fourth subdomain of human (h)TNFr were previously determined with NMR spectroscopy and X-ray crystallography, respectively (Doreleijers *et al.,* 1996; Naismith *et al.,* 1996). NMR-analysis of a 32-residue peptide corresponding to the complete central conserved region of BRSV-G, showed that 19 C-terminal residues form a small rigid core and the N-terminal residues were unstructured in solution. Several X-ray structures have been obtained for hTNFr. However, in contrast to the BRSV-G peptide, in most crystals the C-terminal module of the fourth subdomain was disordered and only the N-terminal module of the fourth subdomain was structured (Banner *et al.,* 1993; Naismith *et al.,* 1996). At high salt concentrations and low pH, crystals were obtained in which the entire protein was well-ordered including the C-terminal module of the fourth subdomain (Naismith *et al.,* 1996). The C-terminal module of the fourth subdomain exhibits a topology and disulfide connectivity that differs from the other TNFr subdomains but was identical to the cystine noose of BRSV-G (Fig. 1).

C-terminal module

Although a general structural similarity between the BRSV-G and TNFr cystine noose is evident, the structural details are different (Fig. 2). The secondary structure for BRSV-G is helix - type 1′ turn - helix. The first small helix in BRSV-G corresponds with a gamma turn in hTNFr, the type 1′ turn in BRSV-G corresponds to a type 2 turn in TNFr (residues KKSL, and is shifted one residue relative to BRSV) and finally, the second helix is only 4 residues in hTNFr (vs. 6 residues in BRSV-G). As a consequence, some important structural details are different. A typical structural feature of the RSV-G module is the conserved pocket which is formed by 7 invariant residues including the cystine bridges (Doreleijers *et al.,* 1996). Strikingly, these are the only residues conserved between the RSV-G and the TNFr cystine noose (Table 1). However, in TNFr the residues are less clustered and do not form the typical pocket. The inner disulfide

bridge of the TNFr noose is right-handed instead of left-handed as in the BRSV-G noose. The backbone RMSD between the two cystine nooses is large (0.25 nm between Val_{171} to Cys_{186}.) However, when the backbone of the TNFr was rotated at residue Cys_{150}, the RMSD of the cystine noose is much smaller. Since the exprimental cystine noose structures were determined under different conditions and with different techniques, a higher similarity of the native structures can not be excluded. The cystine noose of BRSV-G is a solution structure of a synthetic peptide determined by NMR and the cystine noose of hTNFr is a crystal structure of a recombinant protein at low pH and high salt concentration. These different approaches may account for the structural differences. Crystal structures of TNFr at physiological pH and salt concentrations, showed a flexible cystine noose (C2 module) of which the structure could not be determined and some residue sidechains at the interface of the A1 module and the (flexible) C2 module are very different in both types of crystals. Therefore, both domains may structurally be even more similar than the experimental structures suggest.

Molecular dynamics simulations

Molecular Dynamics (MD) simulations in aqueous solution were performed on the cystine nooses of BRSV-G and hTNFr structures to study structural and dynamic features of both modules. Despite inherent limitations of the MD technique such as imperfections in the interatomic interaction functions (force field) and limited sampling time, it can be used as a tool to assess structural stability.

Protein molecules can be expected to adapt their conformation upon transition from a crystal environment to a simulated solution environment. RMSD's from crystallographic structures of 0.1 to 0.2 nm are commonly observed during MD trajectories (e.g. Fox and Kollman, 1996). Figure 3a shows the RMSD from both starting structures of the trajectories of the cystine nooses of BRSV-G and TNFr as a
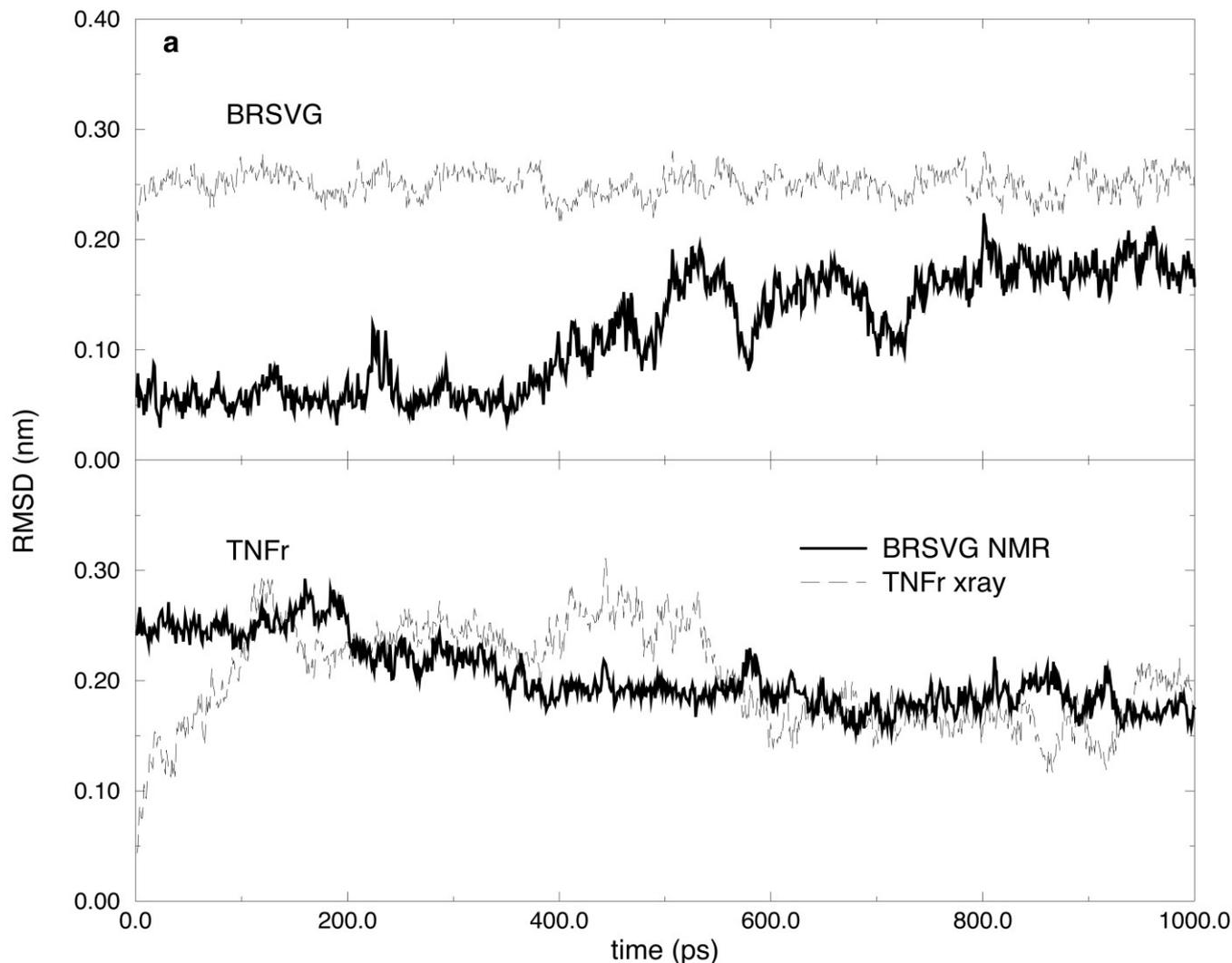
FIG. 3. (a) RMSD to the BRSV-G NMR structure and the TNFr X-ray structure during the simulation of the BRSV-G (upper panel) and TNFr (lower panel) cystine nooses. (b) RMSD to the BRSV-G NMR structure and the TNFr X-ray structure during the simulations of the BRSV-G′ (upper panel) and TNFr′ (lower panel) cystine nooses.

function of time. The BRSV-G structure stays remarkably close to the experimental solution structure for the first 400 ps. In the last half of the 1ns trajectory the structure drifts further away from the NMR structure but the overall structure is well preserved (average RMSD 0.12 nm). During the simulation, there is no tendency to drift towards the backbone conformation of the TNFr X-ray structure. The simulation started from the TNFr X-ray structure shows a clear drift from its starting conformation towards the BRSV-G NMR structure. After 700 ps, the RMSD from the BRSV-G NMR structure is as low as 0.14 nm (the two experimental structures have a backbone RMSD of 0.25 nm). At this point, the RMSD from the TNFr X-ray structure is 0.15 nm, whereas a much higher RMSD (above 0.3 nm) had been encountered before, possibly indicating a transition state.

Models were built for the cystine noose of hTNFr based on the NMR structure of the BRSV-G cystine noose, and a model for the cystine noose of BRSV-G

based on the crystal structure of the fourth subdomain of hTNFr. Both models were simulated to further study whether the two structures are interchangeable. Figure 3b shows the RMSD's with respect to both experimental structures for these trajectories. The BRSV-G sequence modeled onto the TNFr X-ray structure exhibits a drift towards the BRSV-G NMR structure, somewhat comparable to the simulation of the cystine noose of TNFr. The other modeled structure, of the TNFr sequence modeled onto the BRSV-G NMR structure, stays relatively close to its starting conformation (average RMSD of 0.16 nm), suggesting that overall, a conformation close to the NMR structure of BRSV-G is available to the TNFr sequence. The decreasing RMSD with respect to the TNFr X-ray structure indicates that during the simulation, some structural features emerge which are shared with the crystal structure.

In Fig. 4 the secondary structure is plotted as a func-
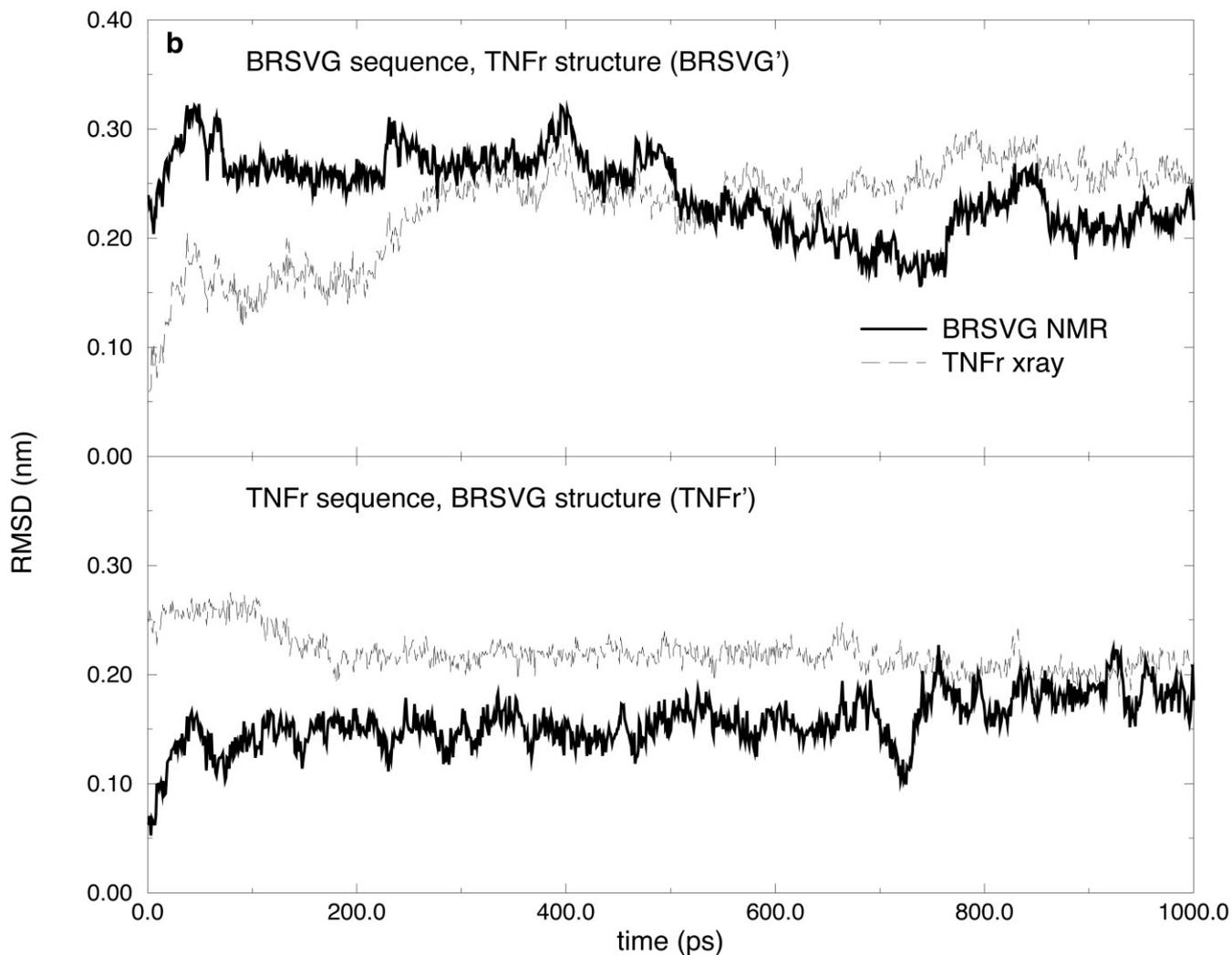
FIG. 3—*Continued*

tion of time for the different simulations. The BRSV-G simulation remains close to its starting conformation but after 400 ps the short N-terminal helix disappears and is replaced by a 3-helix and turn. The TNFr conformations are much less structured. Residues 11 to 15 form an alpha helix or 3-helix however, in the course of the simulation. The simulation of BRSV-G modeled onto the TNFr structure remains unstructured during most of the simulated time and does not find structures close to the BRSV-G NMR structure. TNFr modeled onto the NMR structure of BRSV-G looses the N-terminal helix almost immediately, but the C-terminal helix is maintained during the rest of the simulation.

N-terminal module

Although the C-terminal part of the central conserved region of BRSV-G and the C-terminal module of the fourth subdomain of hTNFr are structurally similar (Figs. 1 and 3), the structural similarity of the N-terminal part with

TNFr is unknown because this part of the peptide was flexible in solution. Although the length of the N-terminal part of the BRSV-G peptide is exactly the same as the A1 module of TNFr, there is no sequence similarity (Table 1). However, sequence similarity is probably not meaningful for the A1 module because generally, very little sequence similarity is observed in the structurally conserved A1 modules. Naismith *et al.* (1996) suggested that the number, rather than the type of amino acid determines the structure of variable loop regions in the A1 module. Therefore, additional to the C-terminal similarity, a structural similarity for the N-terminal part of the alignment can also be expected.

One of the few structurally important residues in the A1 module is a conserved aromatic residue which is conserved in TNFr family members and in many RSV-Gs. This aromatic residue is crucial for domain folding which is involved in the packing of the upper and lower module (A1 and (B2 or C2)) (Banner *et al.*, 1993; Naismith *et al.*, 1996).
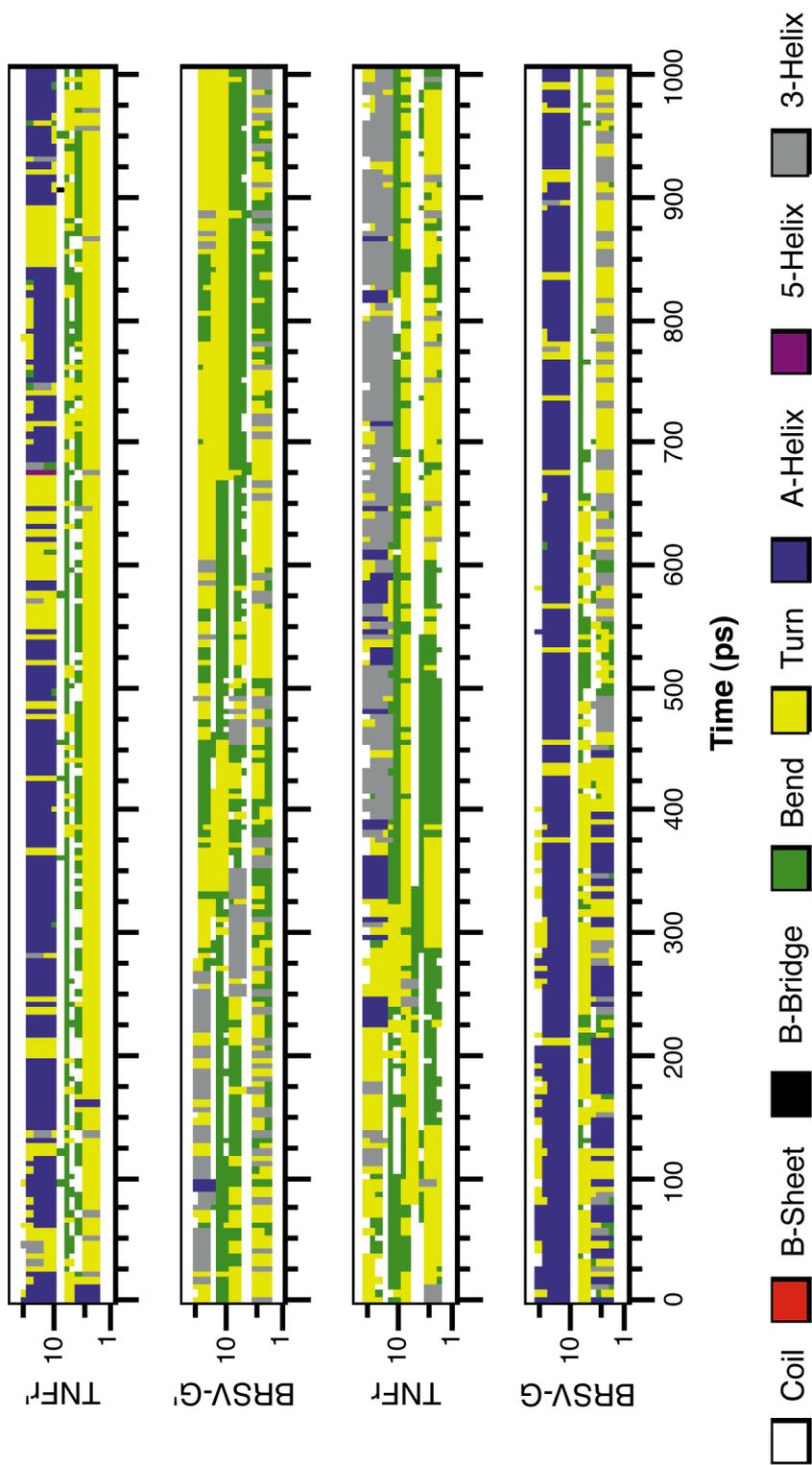
FIG. 4. Schematic representation of the secondary structures of cystine nooses of TNFr', BRSV-G', TNFr and BRSV-G as calculated by DSSP (Kabsch and Sander, 1983) as a function of time for the four MD simulations.
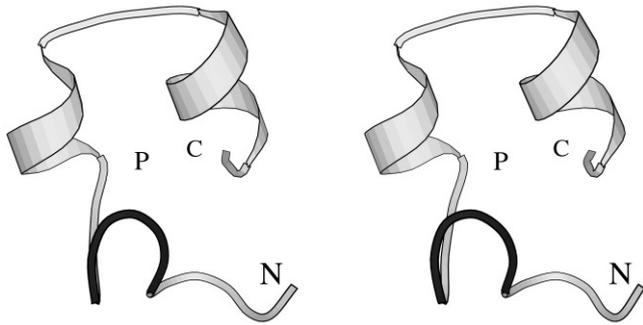
FIG. 5. Stereoview of structural model of complete central conserved region of BRSV-G based on homology modelling with fourth repeat of TNFr. All nonhomologous amino acids of the fourth repeat of hTNFr were replaced by the BRSV-G amino acids according to the alignment of Table 1. Highly conserved region within HRSV-G subtypes (black fills), N- and C-termini (N, C) and location of conserved pocket (P) are indicated. The diagram was generated by Molscript (Kraulis, 1991).

The two Cys residues that are missing in RSV-G according to the alignments (Table 1) belong to the same cystine bridge in 55 kDa TNFr which connects loop 1 in the A1 module (Fig. 1). Additionally, in BRSV-G these Cys residues connecting loop 1 are replaced by His_{159} and Tyr_{170}, two residues that occur frequently in side chain clusters in protein structures (Heringa and Argos, 1991). The relatively large surfaces of His and Tyr can have extensive interactions and the hydroxyl group of Tyr prefers to be in the vicinity of a nitrogen atom in the His side chain (Narayana and Argos, 1984). So, contacts between His_{159} and Tyr_{170} may substitute the lost disulfide bridge. Amino acid substitutions at positions 159 and 170 of other types of RSV-G are all common residues found in side chain clusters except for Pro_{159} of HRSV-G, which occurs infrequently in side chain clusters (Heringa and Argos, 1991).

A model was constructed for the complete central conserved region of BRSV-G based on the structure of the fourth subdomain of hTNFr (Naismith et al., 1996). Amino acids of human TNFr were replaced by homologous amino acids of BRSV-G. For amino acids contained in gap regions according to the alignment, loop searches were performed as described in material and methods. An MD simulation of 10 ps with positional restraints towards the BRSV-G cystine noose was performed to obtain a model based on the TNFr X-ray structure but with structural features of BRSV-G (Fig. 5).

The obtained peptide was simulated without restraints for 1 ns to assess the stability of the model. An analysis of the secondary structure showed that apart from the small N-terminal helix in the noose the structure is stable in the simulated timespan (data not shown). This helix was also found to be unstable in the simulation of the isolated noose (Fig. 4). These results suggest that based on the structure of TNFr a relatively stable model for the N-terminal part of BRSV-G can be built. Based on the

NMR data, however, it is likely that the structure is only metastable, undergoing conformational changes on short timescales.

DISCUSSION

A structural homology is observed between the C-terminal part of the central conserved region of BRSV-G and the C-terminal module of the fourth subdomain of the 55-kDa TNFr. MD simulations showed that both C-terminal cystine nooses are possibly even more similar then their previous structure determinations suggested. The observed drifts (Fig. 3) are probably indicative of a convergence to an equilibrium situation and not the result of low frequency motions in the simulations because for both the TNFr and the BRSV-G cystine noose sequences the average backbone RMSD to the BRSV-G NMR structure is almost 0.05 nm lower than that to the TNFr X-ray structure (Fig 3). This is an average over four independent simulations, which is much less influenced by statistical artefacts than each simulation individually, and therefore seems to be a significant indication that a structure more similar to the BRSV-G NMR than to the TNFr X-ray structure is the most likely conformation for both peptides. The similarity is mostly confined to the N- and C-terminal helical regions of the nooses. During the simulations the type II turn of hTNFr does not drift to the type I' turn which is present in the cystine noose of BRSV-G. However, according to statistical analysis of residue occurrence at particular positions of turns, the $^{157}KKSL^{160}$ sequence of TNFr has a higher type I' turn propensity than type II turn propensity (Wilmot and Thornton, 1988). Furthermore, the present structure of TNFr does not explain the conserved nature of Asn_{159} of mouse, rat and swine TNFrs (Asn^{179} in RSV-Gs) which would be highly exposed in the solution in the type II turn. In RSV-G the conserved nature of Asn^{179} can be explained by its important role in the structure because Asn^{179} stabilizes the second helix and is involved in stabilization of the type I' turn (Doreleijers et al., 1996). We have to await NMR analysis of the complete fourth TNFr subdomain or the X-ray structure of BRSV-G to exactly determine the degree of similarity of both cystine nooses.

Based on homology modelling, a model was constructed for the unresolved N-terminal part of BRSV-G which would make the structure of the central conserved region complete. Although the N-terminal part of the central conserved region is not the most conserved region in RSV-Gs of different species, it does contain the most conserved region between the HRSV-A and B subtypes. Therefore, this region may have an important role in the type-specific binding to a RSV-G receptor. This conserved region of HRSV-G corresponds to loop 1 (Figs. 1 and 5) and clusters together with the "conserved pocket region" on one face of the molecule. However, in the

complete structure (Fig. 5), the "conserved pocket region" is not completely exposed but is partly covered by loop 1 due to packing of the N-terminal A1 module and the cystine noose. If the complete central conserved region and the fourth subdomain of hTNFr, including the A1 module, are structurally similar, then it is still uncertain whether the A1 module and the cystine noose are packed together. Both the solution structure of the BRSV-G peptide and the X-ray structure of the physiological hTNFr crystals suggest that both modules are not tightly associated. However, in the low pH crystals both modules are associated. If the two modules are also associated in solution under physiological conditions, this means that the highly conserved pocket in the flat surface of BRSV-G is not exposed to form a putative receptor binding site (Doreleijers *et al.,* 1996; Langedijk *et al.,* 1997a). Instead, the postulated receptor binding site would be involved in intraprotein interaction. Possibly, the flexibility allows it to perform both functions.

TNFα and the closely related TNFβ are proinflammatory cytokines of major importance (reviewed by Dinarello, 1992). In addition, TNFα is directly cytotoxic to certain infected cells. High concentrations of TNF can induce septic shock and fever (Tracey and Cerami, 1994). Both TNFs compete for binding to each of the two TNF receptors: 55-kDa TNFr and 75-kDa TNFr (reviewed by Loetscher *et al.,* 1991). Cytokines of the TNF ligand family and their cognate receptors, including the 55-kDa TNFr, trigger the cell suicide response (Nagata, 1997).

The 55-kDa TNFr is a member of a large TNF receptor family that encompasses the 75-kDa TNF receptor, the low affinity NGF receptor, CD40, 4-1BB, OX40, Fas CD27 and CD30. In addition to these receptor-type membrane proteins, some viruses of the leporiviridae and the orthopoxviridae contain genes that encode soluble, secreted forms of TNF receptors (Shchelkunov *et al.,* 1993; Smith *et al.,* 1991). Such large DNA viruses have been shown to contain many homologues of immunologically important genes including TNF receptors. The TNFr homologues bind (inactivate) host-produced TNF and are therefore important virulence factors (Upton *et al.,* 1991). Because RSV-G exists as a membrane-bound and a soluble, secreted form (Hendricks *et al.,* 1987; Roberts *et al.,* 1994) it is possible that, analogous to poxviruses, the TNFr-like domain in RSV-G influences the pathogenesis of the infection by modulating the TNF response or the response of an unknown TNF homologue. TNFr homologues in poxviruses which inhibit TNF function share more homology with the high affinity 75-kDa TNF receptor than with the 55-kDa TNFr which has lower affinity for TNFs (Hu *et al.,* 1994). This study describes for the first time that a homology is found for the 55-kDa TNFr and the first time that such a homology is found for an RNA virus. Although a similar function is expected for the fourth domain of TNFr and for the central conserved region of RSV-G, for none of these two domains a func-

tion has been described. According to the crystal structure (Banner *et al.,* 1993), TNFβ binds to TNFr through contacts with subdomains 2 and 3, and TNFα is supposed to bind in a similar fashion. A 55 kD TNFr in which the complete fourth subdomain was deleted, could still bind TNFα (Chen *et al.,* 1995). However, in other studies, peptide mapping suggested that domain 4 is involved in ligand binding, and a monoclonal antibody, specific for the fourth domain could block TNFα induced cell death (Hwang *et al.,* 1991; Lie *et al.,* 1992). Because TNF and TNFr family members are all involved in distinct but overlapping cellular responses such as apoptosis, necrosis and costimulation, the identification of the RSV-G receptor may be a key to the elucidation of RSV induced pathology, but inhibition of TNF activity by RSV-G remains to be proven.

TNF is a very important proinflammatory cytokine with antiviral effect. This importance is compatible with the fact that many viruses have obtained means to block TNF activity. The homology of a unique module in the 55-kDa TNFr with the most conserved module of RSV-G, which can be released as a soluble form, suggests that RSV-G may somehow modulate the activity of TNF or another unknown ligand of the 55-kDa TNFr. The discovered homology will give new directions to future research on the function of the central conserved region of RSV-G and on a neglected part of the 55-kDa TNFr.

MATERIALS AND METHODS

Sequence analysis and molecular modeling

Multiple sequence alignments were performed using several sequences of 55-kDa TNF-receptors and RSV-G family members. The following sequences were obtained from the CAOS CAMM Center in Nijmegen, the Netherlands for comparison: HRSV-G type A, strain RSB642 (accession number P27021), HRSV-G type B, strain 18537 (P20896), ORSV-G (JQ2388), BRSV-G, strain Copenhagen (P22261), human 55-kDa tumor necrosis factor receptor (TNFr) (P19438), mouse 55-kDa TNFr (P25118), rat 55-kDa TNFr (P22934), swine 55-kDa TNFr (P50555).

Molecular modeling was performed using software of SYBYL version 6.2 (Tripos Associates, St. Louis, MO) on a Silicon Graphics Indigo. Energy minimization was performed using the Tripos Sybyl version 6.2 force field. Minimization was performed using a dielectric constant $\epsilon = 1$. Minimization was done in stages using steepest descent and conjugate gradient; each stage the atoms were given more freedom as described (Mackay *et al.,* 1989). For the introduction of insertions and deletions in the model structure, the program LOOP SEARCH in the SYBYL package was used. The loop regions were taken from a protein fragment database and the selection was based on the correct length, maximum amino acid homology and minimum Root Mean Square difference of

the anchor residues in the start and the end of the loop. The N- and C-terminus of all structures were treated as acetyl and amide respectively because they mimic the adjacent uncharged backbone in the native protein. All modelling studies were performed in vacuo, in contrast with the subsequent simulations. Subsequently, the structure was simulated for 10 ps with a harmonical positional restraints towards the BRSV-G cystine noose (force constant of 1000 kJ mol^{-1} nm^{-1}) to obtain a model based on the TNFr X-ray structure but with structural features of BRSV-G. Additional simulations were performed for 1 ns to check whether the peptide structure was stable.

Molecular dynamics simulations

Four simulations were performed on the two cystine nooses corresponding to the underlined sequences in Table 1 and the two cystine noose models, each for one ns. The first simulation started from one of the structures in the NMR cluster of the cystine noose of BRSV-G (first structure of pdb entry 1BRV). The second simulation started from the X-ray structure of the cystine noose of TNFr (pdb entry 1EXT, coordinates of the crystal structure of 55-kDa human TNFr were kindly provided by Dr. James Naismith (St Andrews University, Scotland)). The third simulation started from the BRSV-G sequence modeled onto the TNFr X-ray structure (BRSV-G'). The fourth and final simulation started from the TNFr sequence modeled onto the BRSV-G NMR structure (TNFr').

All simulations were performed in a periodic box filled with approximately 3000 SPC (Berendsen, 1981) water molecules (also crystallographic water molecules were included in the TNFr simulation). Polar and aromatic hydrogens were added to the protein. In the BRSV-G and BRSV-G' simulations one sodium ion and in the TNFr and TNFR' simulations two chloride ions were added to compensate for the net charge on the peptides by replacing water molecules at the lowest, respectively highest electrostatic potential. The simulations were performed at neutral pH (i.e. with neutral histidines) and for the termini we chose to simulate the peptides as zwitterions (NH3$^+$ and COO$^-$ termini).

The simulated systems varied in size between 8000 and 12000 atoms. Prior to simulation, the systems were energy-minimised for 100 steps using a steepest-descents algorithm. Subsequently the systems were simulated for 10 ps with a harmonic positional restraint on all protein atoms (force constant of 1000 kJ mol^{-1} nm^{-2}) for an initial equilibration of the water molecules. Production runs of 1 ns started from the resulting structures. All simulations were run at constant volume. The temperature was kept constant at 300 K by weak coupling to a temperature bath (Berendsen, 1984) (tau = 0.1 ps). A modification (Van Buuren et al., 1993) of the GROMOS87 (Van Gunsteren et al., 1987) was used with additional terms for aromatic hydrogens (Van Gunsteren et al., 1996). SHAKE (Ryckaert et al., 1977) was used to constrain bond lengths, allowing a time step of 2 fs. A twin-range cut-off method was used for non-bonded interactions. Lennard-Jones and Coulomb interactions within 1.0 nm were calculated every step, whereas Coulomb interactions between 1.0 and 1.5 nm were calculated every ten steps. All simulations were performed with the GROMACS simulation package (Van der Spoel et al., 1995).

REFERENCES

Banner, D., D'Arcy, A., Janes, W., Gentz, R., Schoenfeld, H-J., Broger, C., Loetscher, H., and Lesslauer, W. (1993). Crystal structure of the soluble human 55 kd TNF receptor-human TNFa complex: Implications for TNF receptor activation. Cell 73, 431–445.

Berendsen, H. J. C., Postma, J. P. M., Van Gunsteren, W. F., and Hermans, J. (1981). In "Intermolecular Forces, Interaction Models for Water in Relation to Protein Hydration" (B. Pullman, Ed.), pp. 331–342. Reidel, Dordrecht.

Berendsen, H. J. C., Postma, J. P. M., DiNola, A., and Haak, J. R. (1984). Molecular dynamics with coupling to an external bath. J. Chem. Phys. 81, 3684–3690.

Chen, P. C. H., Dubois, C., and Chen, M. J. (1995). Mapping the domains critical for the binding of human tumor necrosis factor α to its two receptors. J. Biol. Chem. 270, 2874–2878.

Devereux, J., Haeberli, P., and Smithies, O. (1984). A comprehensive set of sequence analysis programs for the VAX. Nucleic Acids Res. 12, 387–395.

Dinarello, C. A. (1992). Role of interleuking-1 and tumor necrosis factor in systemic responses to infection and inflammation. In "Inflammation: Basis Principles and Clinical Correlates" (J. I. Gallin, I. M. Goldstein, and R. Snyderman, Eds.), pp. 211–232. Raven Press, New York.

Doreleijers, J. F., Langedijk, J. P. M., Hard, K., Boelens, R., Rullmann, J. A. C., Schaaper, W. M. M., Van Oirschot, J. T., and Kaptein, R. (1996). Solution structure of the immuno dominant region of protein G of bovine respiratory syncytial virus. Biochemistry 35, 14684–14688.

Fox, T., and Kollman, P. A. (1996). The application of different solvation and electrostatic models in Molecular Dynamics simulations of ubiquitin: How well is the X-ray structure "maintained"? Proteins: Structure, Function and Genetics 25, 315–334.

Hendricks, D. A., Baradaran, K., McIntosh, K., and Patterson, J. L. (1987). Appearance of a soluble form of the G protein of respiratory sycytial virus in fluids. J. Gen. Virol. 68, 1705–1714.

Heringa, J., and Argos, P. (1991). Side-chain clusters in protein structures and their role in protein folding. J. Mol. Biol. 220, 151–171.

Hu, F. Q., Smith, C. A., and Pickup, D. J. (1994). Cowpox virus contains two copies of an early gene encoding a soluble secreted form of the type II TNF receptor. Virology 204, 343–356.

Hwang, C., Gatanaga, M., Innins, E. K., Yamamoto, R. S., Granger, G. A., and Gatanaga T. (1991). A 20 amino acid synthetic peptide of a region from the 55 kDa human TNF receptor inhibits cytolytic and binding activities of recombinant human tumour necrosis factor in vito. Proc. R. Soc. Lond. 245, 115–119.

Kabsch, W., and Sander, C., (1983). Dictionary of protein secondary structure: Pattern recognition of hydrogen-bonded and geometrical features. Biopolymers 22, 2577–2637.

Kraulis, P. J. (1991). MOLSCRIPT: A program to produce both detailed and schematic plots of protein structures. J. Appl. Cryst. 24, 946–950.

Langedijk, J. P. M., Schaaper, W. M. M., Meloen, R. H., and Van Oirschot, J. T. (1996a). Proposed three-dimensional model for the attachment protein G of respiratory syncytial virus. *J. of Gen. Virol.* **77**, 1249–1257.

Langedijk, J. P. M., Middel, W. G. J., Schaaper, W. M. M., Meloen, R. H., Kramps, J. A., Brandenburg, A. H., and Van Oirschot, J. T. (1996b). Type-specific serologic diagnosis of repiratory syncytial virus infection, based on a synthetic peptide of the attachment protein G. *J. of Immun. Meth.* **193**, 157–166.

Langedijk, J. P. M., Meloen, R. H., Taylor, G., Furze, J. M., and Van Oirschot, J. T. (1997a). Antigenic structure of the central conserved region of protein G of bovine respiratory syncytial virus. *J. of Virol.* **71**, 4055–4061.

Langedijk, J. P. M., Brandenburg, A. H., Middel, W. G. J., Osterhaus, A., Meloen, R. H., and Van Oirschot, J. T. (1997b). A sybtype-specific peptide-based enzyme immunoassay for detection of antibodies to the G protein of human respiratory syncytial virus is more sensitive than routine serological tests. *J. of Clin. Microb.* **35**, 1656–1660.

Lie, B. L., Tunemoto, D., Hemmi, H., Mizukami, Y., Fukuda, H., Kikuchi, H., Kato, S., and Numao, N. (1992). Identification of the binding site of 55kDa tumor necrosis factor receptor by synthetic peptides. *Bioch. and Bioph. Res. Commun.* **188**, 503–509.

Loetscher, H., Brockhaus, M., Dembic, Z., Gentz, R., Gubler, U., Hohmann, H. P., Lahm, H. W., Van Loon, A. P. G. M., Pan, Y. C. E., Schlaeger, E. J., Steinmetz, M., Tabuchi, H., and Lesslauer, W. (1991). Two distinct tumor necrosis factor receptors: Members of a new cytokine receptor gene family. *Oxford Surv. Euk. Genes.* **7**, 119–142.

Mackay, H. J., Cross, M. J., and Hagler, A. T. (1989). The role of energy minimization in simulation strategies of biomolecular systems. *In* "Prediction of Protein Structure and the Principal of Protein Conformation." (G. D. Fasman, Ed.), p. 340. Plenum, New York.

Nagata, S. (1997). Apoptosis by death factor. *Cell* **88**, 355.

Naismith, J. H., Devine, T. Q., Kohno, T., and Sprang, S. R. (1996). Structure of the extracellular domain of the type I tumor Nucrosis factor receptor. *Structure* **4**, 1251–1262.

Narayana, S. V. L., and Argos, P. (1984). Residue contacts in protein structures and implications for protein folding. *Int. J. Peptide Protein Res.* **24**, 25–39.

Norrby, E., Mufson, M. A., Alexander, H., Houghten, R. A., and Lerner, R. A. (1987). Site directed serology with synthetic peptides representing the large glycoprotein G of respiratory syncytial virus. *Proc. Natl. Acad. Sci. USA* **84**, 6572–6576.

Roberts, S. R., Lichtenstein, D., Ball, L. A., and Wertz, G. W. (1994). The membrane-associated and secreted forms of the respiratory syncytial virus attachment glycoprotein G are synthesized from alternative initiation codons. *J. Virol.* **68**, 4538–4546.

Ryckaert, J. P., Ciccotti, G., and Berendsen, H. J. C. (1977). Numerical integration of the cartesian equations of motion of a system with constraints; Molecular Dynamics of n-Alkanes. *J. Comp. Phys.* **23**, 327–341.

Satake, M., Coligan, J. E., Elango, N., Norrby, E., and Venkatesan, S. (1985). Respiratory syncytial virus envelope glycoproetein (G) has a novel structure. *Nucleic Acids Res.* **13**, 7795–7812.

Shchelkunov, S., Blinov, V., and Sandakhchiev, L. (1993). Genes of variola and vaccinia viruses necessary to overcome the host protective mechanisms. *FEBS Lett.* **319**, 80–83.

Simard, C., Nadon, F., Séguin, C., Thien, N. N., Binz, H., Basso, J., Laliberté, J. F., and Trudel, M. (1997). Subgroup specific protection of mice from respiratory syncytial virus infection with peptides encompassing the amino acid region 174-187 from the G glycoprotein: The role of cysteinyl residues in protection. *Vaccine* **15**, 423–432.

Smith, C. A., Davis, T., Wignall, J., Din, W., Farah, T., Upton, C., McFaddan, G., and Goodwin, R. (1991). T2 open reading frame from the shope fibroma virus encodes a soluble form of the TNF receptor. *Biochem. Biophys. Res. Commun.* **176**, 335–342.

Stott, E. J., and Taylor, G. (1985). Respiratory syncytial virus: Brief review. *Arch. Virol.* **84**, 1–52.

Tracey, K. J., and Cerami, A. (1994). Tumor necrosis factor: A pleiotropic cytokine and therapeutic target. *Annu. Rev. Med.* **45**, 491–503.

Trudel, M., Nadon, F., Séguin, C., and Binz, H. (1991). Protection of BALB/c mice from respiratory syncytial virus infection by immunization with a synthetic peptide derived from the G glycoprotein. *Virology* **185**, 749–757.

Upton, C., Macen, J. L., Schreiber, M., and McFadden, G. (1991). Myxoma virus expresses a secreted protein with homology to the tumor necrosis factor receptor gene family that contributes to viral virulence. *Virology* **184**, 370–382.

Van Buuren, A. R., Marrink, S-J., and Berendsen, H. J. C. (1993). A Molecular Dynamics study of the decane/water interface. *J. Phys. Chem.* **97**, 9206–9212.

Van der Spoel, D., Berendsen, H. J. C., Van Buuren, A. R., Apol, E., Meulenhoff, P. J., Sijbers, A. L. T. M., and Van Drunen, R. (1995). "Gromacs User Manual." Nijenborgh 4, 9747 AG Groningen, The Netherlands. Internet: http://rugmd0.chem.rug.nl.

Van Gunsteren, W. F., and Berendsen, H. J. C. (1987). "Gromos User Manual." Biomolecular Software, Laboratory of Physical Chemistry, University of Groningen, The Netherlands.

Van Gunsteren, W. F., Billeter, S. R., Eising, A. A., Hünenberger, P. H., Krüger, P., Mark, A. E., Scott, W. R. P., and Tironi, I. G. (1996). "Biomolecular Simulation: The GROMOS96 Manual User Guide." Organization Biomos b.v., Zürich, Groningen.

Wertz, G. W., Collins, P. L., Huang, Y., Gruber, C., Levine, S., and Ball, L. A. (1985). Nucleotide sequence of the G protein of human respiratory syncytial virus reveals an unusual type of viral membrane protein. *Proc. Natl. Acad. Sci. USA* **82**, 4075–4079.

Wilmot, C. M., and Thornton, J. M. (1988). Analysis and prediction of the different types of B-turn in proteins. *J. Mol. Biol.* **203**, 221–232